International Journal of Pure and Applied Mathematics

Volume 32 No. 1 2006, 1-22

NUERBS FORM OF EXPO-RATIONAL B-SPLINES

Lubomir T. Dechevsky[1] §, Arne Laksås[2], Børre Bang[3]

[1,2,3]R&D Group for Mathematical Modelling,
Numerical Simulation and Computer Visualization
Institute for Information, Energy and Space Technology
Narvik University College
2 Lodve Lange's St.
P.O. Box 385, Narvik, N-8505, NORWAY
[1]e-mail: ltd@hin.no
url: http://ansatte.hin.no/ltd/
[2]e-mail: ala@hin.no
url: http://ansatte.hin.no/ala/
[3]e-mail: bb@hin.no
url: http://ansatte.hin.no/bb/

Abstract: We introduce the several possible "NUERBS" forms of expo-rational B-splines, and discuss the hierarchy of these forms in the univariate case. We give some first instances of exploration of properties of the expo-rational NUERBS which depend not only on the NUERBS weights but also on the intrinsic parameters of the expo-rational B-splines.

AMS Subject Classification: 65D07, 33A10, 33E20, 33F05, 41A15, 41A30, 44A20, 65D18, 65Y25, 68U05

Key Words: B-spline, Bezier form, rational form, non-uniform rational B-spline (NURBS), non-uniform expo-rational B-spline (NUERBS), special function, Hermite interpolation, Pade interpolation, Taylor series, Laurent series, curve, surface, tensor product

Received: May 28, 2006

§Correspondence author

1. Introduction

This article is an updated and upgraded version of the invited (unpublished) report of the authors at the international workshop eVITA('eVITenskap og Anvendelser (e-Science and Applications): Research in a New Epoch'), held at Simula Research Laboratory, Oslo, Norway, in May 2004 (see also [3]).

Polynomial-based functions, curves and surfaces have traditionally been used in freeform design and in approximating solutions of ordinary and partial differential equations, but these descriptions are bounded by numerous limitations. Four different reasons for these limitations can be described as follows:

(a) For many geometrical applications polynomial growth is not fast enough, resulting in relatively slow "bending" of the functional curves and slow rates of convergence in interpolation and quasi-interpolation processes.

(b) For curves with vector or point coefficients the speed and accelerations of the parametrization are relatively small; this imposes constraints on the sets of point data that these curves can fit well. The same constraints are valid, mutatis mutandis, for parametrization corresponding to kinematical and dynamical systems. For instance, relatively simple dynamical systems that are described by linear systems of ODE with constant coefficients have algebraic polynomial solutions only in very special cases (namely, only when the respective characteristic equations have eigenvalue 0 with multiplicity higher than 1). In the remaining cases the non-periodic solutions have exponential growth.

(c) Polynomials are not compactly supported curves. When designing polynomial-based compactly supported curves (e.g. polynomial B-splines), the C^∞-smoothness of the polynomial is lost, and smoother B-splines must have larger support. Thus, only the piecewise linear B-splines generate tri-diagonal stiffness matrices when used as finite elements. But these B-splines are not even C^1-smooth, and can therefore be used in Galerkin finite element methods only if the respective differential equation is of order at most 2. Smoother B-splines still generate band-limited stiffness matrices, but their bandwidth increases with the increasing smoothness of the polynomial B-spline (note that the essence of these limitations is again in the "slow bending" of the polynomial curve).

(d) In Hermite interpolation (and in related quasi-interpolation involving regularization of interpolation functionals), if $l_j(f) = f^{(j)}(x_0)$, $j = 0, 1, ...$ are the Hermite interpolation constraints, a polynomial spline basis $\{S_k\}$ will typically satisfy

$$\frac{d^j}{dt^j} S_k(t)|_{t=t_0} = \delta_{kj} \tag{1}$$

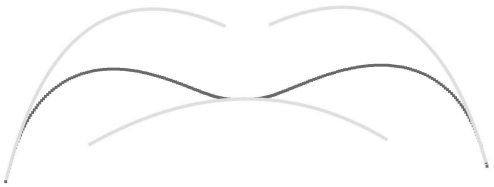

Figure 1: Three local curves and the blended total curve

only for $j \leq m$ and $k \leq m$ for some $m < \infty$, where δ_{kj} is Kronecker's delta (higher order derivatives would not exist or, if existing, would not satisfy (1)). Thus, polynomial-based interpolants are exact only on respective finite spaces of polynomials. Certainly, these problems have been addressed in the literature, and other types of approximation approaches have been proposed in order to outperform polynomial-based curves and surfaces, notably, rational functions and exponential splines (e.g. Euler splines). In particular, NURBS, the rational form of polynomial B-splines, is currently the industrial standard in curve and surface modelling. However, even NURBS has some limitations inherited from the underlying piecewise polynomial curves used to generate the rational form. For example, NURBS are not C^∞-smooth and are exact only in certain finite-dimensional spaces, possibly broader, but still finite-dimensional.

To address all these problems, in [2, 1, 3, 6] we have proposed a new type of B-splines: the expo-rational B-splines. This name reflects the essence of the new idea: rather than taking rational or exponential functions in separate, we use composition of both of these to derive a new B-spline which "bends very fast", has the well-localized support of a linear B-spline while at the same time is C^∞-smooth, generate basis satisfying (1) for all $i = 0, 1, ...,$ and $j = 0, 1, ...,$ and as a consequence generates a basis which is exact on the infinite dimensional space of all entire analytic functions defined on its domain. In other words, each of the aspects (a)-(d) is being addressed simultaneously.

An expo-rational B-spline (ERBS) function or curve is described by:

$$C(t) = \sum_{i=1}^{n} c_i(t) B_i(t)\,, \tag{2}$$

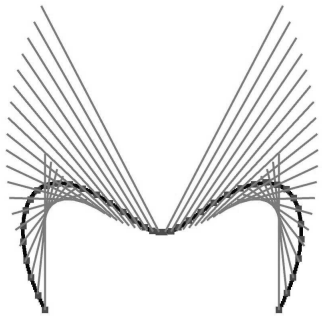

Figure 2: An expo-rational B-spline curve and its moving control polygon (see also [1], Figure 2)

where

$$B_k(t) = \begin{cases} \int\limits_{t_{k-1}}^{t} \varphi_{k-1}(s)ds, & t_{k-1} < t \leq t_k\,, \\ 1 - \int\limits_{t_k}^{t} \varphi_k(s)ds, & t_k < t < t_{k+1}\,, \\ 0, & \text{else}\,, \end{cases} \tag{3}$$

where

$$\varphi_k(t) = \frac{e^{-\beta_k \frac{[t-((1-\lambda_k)t_k+\lambda_k t_{k+1})]^{2\sigma_k}}{((t-t_k)(t_{k+1}-t)^{\gamma_k})^{\alpha_k}}}}{\int_{t_k}^{t_{k+1}} e^{-\beta_k \frac{[s-((1-\lambda_k)t_k+\lambda_k t_{k+1})]^{2\sigma_k}}{((s-t_k)(t_{k+1}-s)^{\gamma_k})^{\alpha_k}}} ds}\,, \tag{4}$$

and

$$\alpha_k > 0, \quad \beta_k > 0, \quad \gamma_k > 0, \quad 0 \leq \lambda_k \leq 1, \quad \sigma_k \geq 0,$$

and where $c_i(t), \quad i = 1, ..., n,$ describe local scalar functions or vector-valued curves. The basis functions $B_k(t)$ are defined by three knots t_{k-1}, t_k, t_{k+1} on a knot vector $\overline{t} = \{t_0, ..., t_{n+1}\}$. A multiple knot is indicative of discontinuity (see [6]), and it follows that $B_i(t) \geq 0, \quad i = 1, ..., n$ and $\sum_{i=1}^{n} B_i(t) = 1$. The default is $\alpha_k = \beta_k = \gamma_k = \sigma_k = 1, \quad \lambda_k = \frac{1}{2}$.

For self-consistency, here we review briefly several relevant observations made in the fundamental paper [2, 1]. The expo-rational B-spline can be viewed as a blending of local functions (curves/surfaces). Figure 1 shows an example

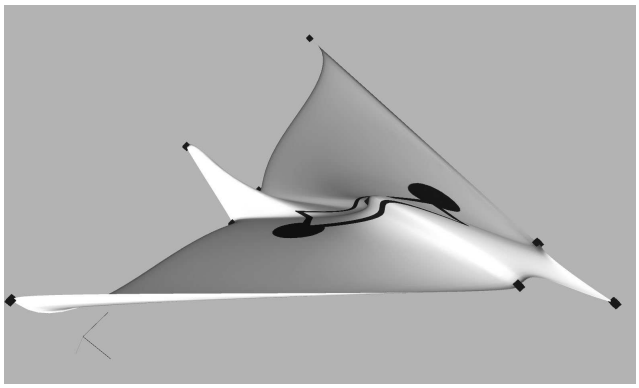

Figure 3: A surface from expo-rational B-splines obtained by editing a plane surface only by moving the 9 local patches. You can see 9 control points (blue cubes) representing local patches. The surface can be edited further by either transforming the local patches or by editing the control polygon of the local patches. The blue texture has originally been marking the boundary of a rectangle in the plane subject to editing (compare also with [1], Figures 4 and 14 and [6], Figure 7)

of a curve and its local blending curves. If we consider the control polygon of a curve/surface, then expo-rational B-splines will have a moving control polygon which is a moving linear segment (because only two neighbouring B-splines are non-zero locally for each t). Figure 2 shows an example of a moving control polygon.

For tensor-product surfaces we have the following formula

$$S(u,v) = \sum_{i=1}^{n} \sum_{j=1}^{m} s_{ij}(u,v) B_i(u) B_j(v), \tag{5}$$

where $s_{ij}(u,v), \quad i = 1, ..., n \quad j = 1, ...m$, are $n \times m$ local patches of arbitrary form. Figure 3 shows an example of an expo-rational surface. The "airplane" is edited from a plane only by moving the local patches. Without going into details about the case of surfaces here, let us note that (5) is exact on an infinite-dimensional space (which is typical, in general, for all blending surfaces). Studying the expo-rational surfaces from the point of view of Gordon surfaces and Boolean sums of projections is of considerable interest, and this extends naturally to the NUERBS forms introduced in the next section.

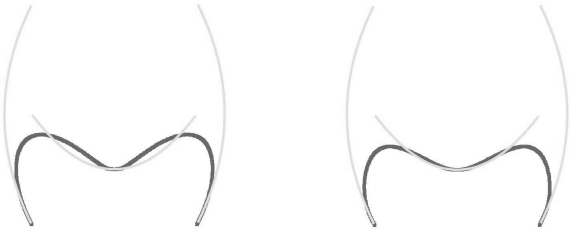

Figure 4: The two curves are equal except that all weights on the left curve are 1, while the middle weight in the curve to the right is 5. Observe that this causes the curve to be pulled towards the middle local curve

2. General NUERBS Form in the Univariate Case

In the following we are going to describe the rational forms of expo-rational B-splines. We shall call these "Non-Uniform Expo-Rational B-splines" (NUERBS), because of the close analogy with NURBS.

The *general NUERBS form* is:

$$f(t) = \frac{\sum_{i=1}^{n} c_i(t) W_i B_i(t)}{\sum_{i=1}^{n} W_i B_i(t)}, \tag{6}$$

where $c_i(t)$, $i = 1, ..., n$ are local curves, scalar or vector-valued. The formula resembles a usual rational Bezier/NURBS. The effect of the weights is also similar to what we expect from rational Bezier/NURBS, except that $c_i(t)$ is not a point but a curve. In Figure 4 is displayed the effect of increase of one weight: the global curve approximates better the corresponding local curve.

If we replace the local curves with points, which corresponds to Lagrange interpolation by B_i at the simple knot t_i, the total curve will geometrically be a piecewise linear curve. Since the curve is infinitely smooth, all derivatives must be zero at each knot. This can be seen in Figure 5 because the points are very dense at the knots (dense means slow speed). The effect of changing the weight is that the dense area is moving. The dense area is getting smaller at the knot with a small weight and bigger at a knot with a bigger weight. In Figure 5 this can be seen on curve b and c. We shall discuss this remarkable phenomenon in

more detail in Section 5.

Remark. The general NUERBS form has variation-diminishing properties for a very broad range of classes of local curves. However, since these properties are a consequence of the variation-diminishing properties of the underlying expo-rational B-splines, it is more appropriate to consider variation diminshing as part of the theory of expo-rational B-splines (see [7] for a discussion of this topic concerning Bezier and B-spline curves, and [2, 1] for the expo-rational case).

2.1. Hermite Interpolation Property of the General NUERBS Form

Here we shall show that under very general assumptions about the class of local curves in (6), the general NUERBS form has an Hermite interpolation property. The important underlying fact here is that

$$\frac{d^j}{dt^j}B_i(t_k) = 0, \quad i = 1, ..., n, \quad k = 0, ..., n+1, \quad j = 1, 2, ..., \tag{7}$$

which was discussed in [2, 1].

Theorem 1. *Let $\overrightarrow{f}_i : [t_{i-1}, t_{i+1}] \to \mathbb{R}^{d_i}, 1 \le d_i < \infty$, be a sequence of C^{m_i}-smooth functions on $[t_{i-1}, t_{i+1}]$, where $m_i \ge 0$ is an integer with $m_i \le \infty$ (in the case of $m_i = \infty$ we assume that f_i is an entire analytic function on $[t_{i-1}, t_{i+1}]$), and consider the weight $W_i \in (0, \infty), i = 1, ..., n$ (where t_i may also be an infinite sequence, $i = 0, \pm 1, \pm 2, .., n = \infty$). Let*

$$\overrightarrow{\Phi}(t) = \frac{\sum_{i=1}^{n} \overrightarrow{f_i}(t) W_i B_i(t)}{\sum_{i=1}^{n} W_i B_i(t)} \tag{8}$$

be the general NUERBS form (6) for $\overrightarrow{f}_i(t), i = 1, ..., n$. Then,

$$\overrightarrow{\Phi}|_{(t_i, t_{i+1})} \in C^{\min(n_i, n_{i+1})}((t_i, t_{i+1}), \mathbb{R}^{\max(d_i, d_{i+1})}), \quad i = 0, .., n, \tag{9}$$

and

$$\frac{d^j}{dt^j}\overrightarrow{\Phi}(t_i) = \frac{d^j}{dt^j}\overrightarrow{f}_i(t_i), \quad j = 0, .., n_i, \quad i = 1, .., n. \tag{10}$$

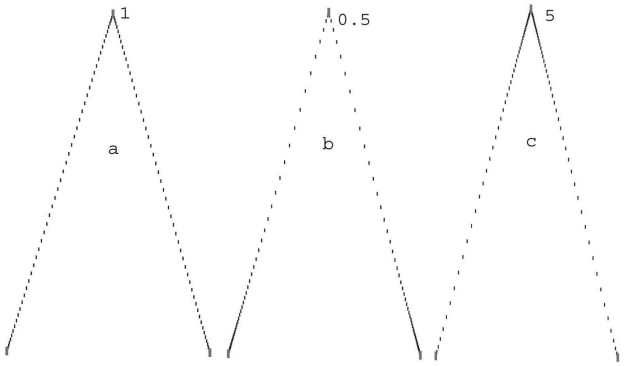

Figure 5: Three piecewise linear curves a, b and c. All weights for curve a are equal to 1, curve b has weight 0.5 in the middle and curve c has weight 5 in the middle (for an alternative set of weights, see also the top level of Figure 10 in [1])

Proof. (Outline) (9) follows immediately from (8), in view of the properties of B_i and the theorem's assumptions about $\overrightarrow{f_i}$. To prove (10), we write (8) in the form

$$(\sum_{i=1}^{n} W_k B_k(t))\,\overrightarrow{\Phi}(t) = \sum_{i=1}^{n} \overrightarrow{f}_k(t) W_k B_k(t) \tag{11}$$

and set $t = t_i$. From the properties of $B_i(t)$, (11) becomes $W_i \overrightarrow{\Phi}(t) = \overrightarrow{f}_i(t) W_i$, from where, since $0 < W_i < \infty$ holds, we get (10) for $j = 0$. Next, we differentiate (11) in t and apply (7) for $j = 1$. From here it is easy to obtain (10) for $j = 1$ by using the already established result (10) for $j = 0$. The general case of (10) is now obtained by induction, using (10) as induction hypothesis for every $j = 0, ..., \nu \leq n_i - 1$, and then also using (7) on the induction step $j = \nu + 1$. We omit the details. □

We will now investigate in more detail the particular case of local polynomial-based curves.

2.2. Local (Algebraic) Polynomial Curves

We shall consider here two different polynomial-based local curves: Hermite interpolants

$$f(t)=\frac{\sum_{i=1}^{n}\sum_{j=0}^{k_i}p_{ij}T_j(\frac{t-t_{i-1}}{t_{i+1}-t_{i-1}})W_iB_i(t)}{\sum_{i=1}^{n}W_iB_i(t)}, \tag{12}$$

where

$$T_j(x)=\frac{x^j}{j!} \tag{13}$$

is the Taylor monomial basis, and Bernstein-Bezier type

$$f(t)=\frac{\sum_{i=1}^{n}\sum_{j=0}^{k_i}c_{ij}b_{k_i,j}(\frac{t-t_{i-1}}{t_{i+1}-t_{i-1}})W_iB_i(t)}{\sum_{i=1}^{n}W_iB_i(t)}, \tag{14}$$

where

$$b_{k_i,j}(x)=\left(\begin{array}{c}k_i\\ j\end{array}\right)x^j(1-x)^{k_i-j}. \tag{15}$$

Our current application is to generate a curve/surface by using Hermite interpolation, then transform it to Bezier type, and then do editing on the geometry.

3. The Hierarchy of General NUERBS Forms of Bernstein-Bezier Type in the Univariate Case

When using polynomial-based local curves, it is possible, of course, to use also the rational form of these curves. In this case we have several alternatives of expanding the expo-rational B-splines into NUERBS. We will now compare 3 different forms of NUERBS based on local rational Bezier curves.

First we look at what we call the *local NUERBS form*:

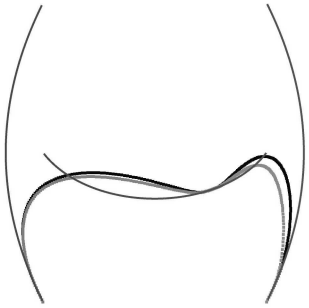

Figure 6: Two global curves based on the same local curves and with all respective weights being the same. The black/outer one is defined via global NUERBS form, the inner one is defined via the local NUERBS form (see Section 3)

$$f(t) = \frac{\sum_{i=1}^{n} \frac{\sum_{j=0}^{k_i} c_{ij} w_{ij} b_{k_i,j}(\frac{t-t_{i-1}}{t_{i+1}-t_{i-1}})}{\sum_{j=0}^{k_i} w_{ij} b_{k_i,j}(\frac{t-t_{i-1}}{t_{i+1}-t_{i-1}})} W_i B_i(t)}{\sum_{i=1}^{n} W_i B_i(t)}. \tag{16}$$

This form is identical with the general NUERBS form where the local curve is a rational Bezier curve.

The second one is the *global NUERBS form*:

$$f(t) = \frac{\sum_{i=1}^{n} \sum_{j=0}^{k_i} c_{ij} \vartheta_{ij} b_{k_i,j}(\frac{t-t_{i-1}}{t_{i+1}-t_{i-1}}) W_i B_i(t)}{\sum_{i=1}^{n} \sum_{j=0}^{k_i} \vartheta_{ij} b_{k_i,j}(\frac{t-t_{i-1}}{t_{i+1}-t_{i-1}}) W_i B_i(t)}. \tag{17}$$

The main difference between this and the local form is that we relate the denominators of the local and global parts, in other words, we consider the two-index basis $\{b_{k_i,j} B_i\}$ as a global basis. The effect of this can be seen on Figure 6. In Figure 6 we have changed the weight on the right endpoint of the second curve to 4, all the other weights, both local and global, are 1. As seen, the global

form is responding more to the increase in weight than the local form. If we change some of the global weights then both forms will respond equally.

Finally, we take a look at what we call the *full NUERBS form*:

$$f(t)=\frac{\sum\limits_{i=1}^{n}\frac{\sum\limits_{j=0}^{k_i}c_{ij}\mu_{ij}\vartheta_{ij}b_{k_i,j}(\frac{t-t_{i-1}}{t_{i+1}-t_{i-1}})}{\sum\limits_{j=0}^{k_i}\vartheta_{ij}b_{k_i,j}(\frac{t-t_{i-1}}{t_{i+1}-t_{i-1}})}W_iB_i(t)}{\sum\limits_{i=1}^{n}\frac{\sum\limits_{j=0}^{k_i}\mu_{ij}\vartheta_{ij}b_{k_i,j}(\frac{t-t_{i-1}}{t_{i+1}-t_{i-1}})}{\sum\limits_{j=0}^{k_i}\vartheta_{ij}b_{k_i,j}(\frac{t-t_{i-1}}{t_{i+1}-t_{i-1}})}W_iB_i(t)}. \tag{18}$$

It can be seen that both the local and the global form are particular cases of the full form. Namely, the full form reduces to the local form when $\mu_{ij}\equiv 1$, and to the global form when $\vartheta_{ij}\equiv 1$; If $\mu_{ij}\equiv\vartheta_{ij}\equiv 1$, we get a particular instance of the general form.

Remark. If in (16)-(18) we choose

$$c_{ij}=\Phi((1-\frac{j}{k_i})t_{i-1}+\frac{j}{k_i}t_{i+1}) \tag{19}$$

for some C^0-regular function Φ defined on $[t_1,t_n]$, we obtain expo-rational B-spline and NUERBS forms of all considered types for the classical Bernstein polynomial operator. Note that this is also a first, particularly simple, instance of a variation diminishing operator (see [7]) in terms of expo-rational B-spline and NUERBS form (see [1]).

Remark. As with expo-rational B-splines, it is easy to generate NUERBS for a closed curve. For this purpose one may start with the Hermite interpolation form of the local polynomial-based curves where the dimensions n_0 and n_m and the interpolation values (1) for the first point t_1 and the last point t_n must be equal, respectively. The next step is conversion to Bernstein-Bezier form of desired NUERBS form. It is possible to achieve all this also directly, by using the interpolation property of the general NUERBS form and proceeding as above in points t_1 and t_n. It is possible also to simply identify the knot t_1 and t_n (cycling of the index i) (knot t_0 and t_{n+1} are ignored in this consideration).

4. Other Instances of the (Non-Algebraic) General NUERBS Form

In this section we shall look briefly at other alternatives to Hermite and Bernstein-Bezier local polynomial curves.

In the first place, there is a diversity of the local polynomial curves which can be used with the expo-rational B-splines and the general NUERBS form. For example, instead of requiring exactness of the interpolation for a polynomial space of maximal dimension, we may use part of $\overrightarrow{c}_{ij}$ to minimize the error remainder by Sard's method (see, e.g., [9]). It is possible to use also orthogonal polynomials with respect to integral weights induced on $[t_k, t_{k+1}]$ by the two adjacent expo-rational B-splines, and so on.

Let us now consider some other classes of local curves which are not algebraic polynomial-based. In this case the local curves f_k are, as follows:

(a) *Trigonometric polynomials.*

$$\overrightarrow{f}_k(t) = \sum_{\mu=0}^{M_k} \overrightarrow{c}_{k\mu} \cos 2\mu\pi\left(\frac{t-t_{k-1}}{t_{k+1}-t_{k-1}}\right) + \sum_{\nu=1}^{N_k} \overrightarrow{c}_{k\nu+M_k} \sin 2\nu\pi\left(\frac{t-t_{k-1}}{t_{k+1}-t_{k-1}}\right), \quad (20)$$

where $n_k = M_k + N_k + 1$. Note that, in general, the resulting expo-rational B-spline and NUERBS curve will not be periodic.

(b) *More general polynomial/trigonometric/exponential expressions.*

$$\overrightarrow{f}_k(t) = \sum_{\mu=0}^{M_k} \left(\sum_{\nu=0}^{N_{k\mu}} \overrightarrow{c}_{k\mu\nu} t^\nu\right) e^{i\xi_\mu t} e^{\eta_\mu t}, \quad (21)$$

where i is the imaginary unit, ξ_μ, η_μ are real numbers, $\mu = 0, ..., M_k$, and $n_k = \sum_{\mu=0}^{M_k} N_{k\mu} + M_k + 1$.

(c) *L-splines.* Case (b) (and its particular sub-case (a)) are instances of solutions of ODE. More generally, in (3) and (6), we may consider L-splines.

(d) *Rational functions.*

$$\overrightarrow{f}_k(t) = \frac{\sum_{\mu=0}^{M_k} \overrightarrow{a}_{k\mu} t^\mu}{\sum_{\nu=0}^{N_k} b_{k\nu} t^\mu}, \tag{22}$$

where $b_{k\nu}$ are scalars, $\nu = 0, ..., N_k$, and where $n_k = M_k + N_k + 2$ (and some constraints on the coefficients $\overrightarrow{a}_{k\mu}, b_{k\nu}$ apply).

(e) *Multilevel expo-rational B-splines.* A particular case of these are expo-rational multi-wavelets (see also [1]), which were first proposed by L.T. Dechevsky and introduced in a joint communication by L.T. Dechevsky, E. Quak, N. Grip, J. Gundersen, A. Lakså, B. Bang and T.N. Moguchaya at the conference *Mathematical Methods for Curves and Surfaces*, Tromsø, 2004.

(f) *Special functions.* Euler splines, Bessel functions, radial-basis functions in the case of surfaces, orthogonal polynomials with respect to the integral weight function generated on $[t_{k-1}, t_{k+1})$ by the ERBS $B_k(t)$, etc.

(g) *Taylor and Laurent series.* If the interpolated function is analytic on (t_{k-1}, t_{k+1}), the Hermite interpolatory properties of the Taylor polynomials extend to the case of the Taylor series. There is also an extension in a different direction to the more general case when the "interpolated" function may have a pole of certain multiplicity in t_k: in this general case the Taylor polynomials extend to rational functions represented in the form of a truncated Laurent expansion. If the function is analytic on (t_{k-1}, t_k) and (t_k, t_{k+1}) but not at t_k (where it can have a pole of finite multiplicity or an essential singularity (e.g., of the type $\exp(|t - t_k|^{-\mu})$, $\mu > 0$) then the truncated Laurent expansion can be replaced by a full Laurent expansion around t_k, valid in (t_{k-1}, t_k) and (t_k, t_{k+1}).

(h) *Functions of a complex variable and functions of several variables.* Multivariate tensor-product ERBS and multivariate ERBS on simplectificated domains were already considered in [2, 1]. In the bivariate case (and, more generally, the case of even number of real variables) it is possible to introduce ERBS of one (or several) complex variable(s) and respective local functions of this (or these) complex variable(s). In the case of triangulations (simplectifications) the construction of the ERBS is the main technical challenge: once the ERBS construction is completed, the extensions to NUERBS forms are relatively straightforward.

Within the classes considered in (a)-(f) there are both interpolatory and Bernstein-Bezier type bases of local curves. A typical example of the former is the Padé approximant in (d) which is known to outperform the Hermite

interpolatory system of polynomials (13) and is of big interest in connection with NUERBS. A typical example of Berstein-Bezier type are the multilevel NUERBS generated in (e). These are also of considerable interest in connection with NUERBS.

Remark. The hierarchy of NUERBS forms described here corresponds to one variable (one scalar real argument), i.e., to parametric curves. For functions of n variabls, $n > 1$, e.g., $n = 2$ for parametric surfaces, $n = 3$ for parametric volume deformations, etc., the respective hierarchies become more complex, but so that the respective hierarchies for lower values of $n_1 = 1, 2, \ldots, n-1$, are nested within the hierarchy for $n_1 = n$, and correspond to "main branches" in the graph tree of the hierarchy for $n_1 = n$. If we consider tensor-product surfaces, volume deformations, etc., this "nesting" of the hierarchies is relatively simple and corresponds to cartesian products of the hierarchies for the lower numbers of variables. On the other hand, for surfaces on triangulations, volume deformations on "tetrahedronizations", etc. (see formulae (55)-(67) and Figures 5-9 in [1]) the "nesting" of the hierarchies of NUERBS forms is organized differently, following the iterative structure of the simplex in $\mathbb{R}^n$. In this case, the hierarchy for $n_1 < n$ corresponds to a "stem subtree" of the tree of the hierarchy for n. It is very important to note here that the very definition of ERBS on triangulated surfaces ($n = 2$), and, more generally, any "simplectificated" manifolds for arbitrary n (number of variables) is already formulated in terms of a NUERBS form (see formulae (55)-(57) in [1]).

5. Basic Differential Geometry of NUERBS

Studying the intrinsic geometry (curvature and torsion) of parametric regular Bezier curves is particularly simple in the endpoints (see [4]). For intermediate values of the Bezier curve parameter, the intrinsic geometry of the curve can be considered as an interpolation of the geometry at the endpoints which depends on the control polygon. The situation is the same with the rational Bezier form (see [4]) where the weights of the rational form add additional fine control over the interpolation of the geometry between the endpoints. In the case of B-splines and NURBS the situation is the same between every two (different) neighbouring knots; thus, the enhancement in the control of the intrinsic geometry of the B-spline and the NURBS curve compared to the Bezier and rational Bezier curve is due to the increase of the number of knots and the control of their position and multiplicity. This is an essential improvement in the control over the curve geometry, in view of the simple dependence of the curvature and

torsion on the NURBS weights in the knots (see [4]).

Like with B-splines and NURBS, the intrinsic geometry of expo-rational B-splines and NUERBS curves is simplest to study in the knots (see [2, 1]).

The first important new observation for regular NUERBS curves is that in the knots the intrinsic geometry of the global curve depends only on the intrinsic geometry of the local curve, i.e., it depends neither on the intrinsic parameters of the expo-rational B-spline basis function, nor on the global weights W_i in (8). More precisely, there holds the following result.

Theorem 2. *Let t_i be one of the knots in (8) and assume that the respective local curve $\overrightarrow{f_i} : [t_{i-1}, t_{i+1}] \to \mathbb{R}^d$ satisfies the following:*

(i) either $d = 1, 2$ and $\overrightarrow{f_i} \in C^2[t_{i-1}, t_{i+1}]$, or $d = 3$ and $\overrightarrow{f_i} \in C^3[t_{i-1}, t_{i+1}]$;

(ii) $\overrightarrow{f_i}$ is regular at t_i, i.e., $\dot{\overrightarrow{f_i}}(t_i) \neq 0$.

Then, for the curvature κ of the (global) NUERBS curve (8),

$$\kappa(t_i) = \frac{\left|\dot{\overrightarrow{f_i}}(t_i) \times \ddot{\overrightarrow{f_i}}(t_i)\right|}{\left|\dot{\overrightarrow{f_i}}(t_i)\right|^3} \tag{23}$$

holds, and for the torsion τ of the (global) NUERBS curve

$$\tau(t_i) = \begin{cases} 0, & d = 1, 2\,, \\ \dfrac{\left[\dot{\overrightarrow{f_i}}(t_i), \ddot{\overrightarrow{f_i}}(t_i), \dddot{\overrightarrow{f_i}}(t_i)\right]}{\left|\dot{\overrightarrow{f_i}}(t_i) \times \ddot{\overrightarrow{f_i}}(t_i)\right|^2}, & d = 3 \end{cases} \tag{24}$$

is fulfilled, where $\overrightarrow{a} \times \overrightarrow{b}$ is the vector cross product of $\overrightarrow{a}$, $\overrightarrow{b}$, and $[\overrightarrow{a}, \overrightarrow{b}, \overrightarrow{c}]$ is the scalar triple product of $\overrightarrow{a}$, $\overrightarrow{b}$, $\overrightarrow{c}$. In particular, $\kappa(t_i)$ and $\tau(t_i)$ depend neither on the weight W_i, nor on the intrinsic parameters of B_i in (8).

Proof. (Outline) Follows from Theorem 1. □

Remark. In the particular case of (18), $\kappa(t_i)$ in (23) and $\tau(t_i)$ in (24) essentially depend, and can be controlled, by the weights ϑ_{ij} of the local rational Bezier curve.

The second important observation about the geometry of NUERBS is that the much faster speeds and accellerations of the parametrization of NUERBS, and the fact that the expo-rational B-Splines are not regular curves at the knots, bring about new qualitative phenomena, as far as geometric continuity

is concerned. A most conspicuous (and practically important) example in this respect is the case of Lagrange interpolation by B_i in (2) and (6), (8). This corresponds to $\overrightarrow{c}_i(t) = \overrightarrow{c}_i$ =const., $t \in [t_{i-1}, t_{i+1}]$. In this case, $|\overrightarrow{f}_i(t)| \neq 0$ for every i, condition (ii) is violated and Theorem 2 does not hold. The effect is that here (2),(6),(8) provide the geometry of a piecewise linear B-spline curve (see Figure 6) while retaining C^∞-smooth parametrization. In this case, the NUERBS weights W_i in (8) do not influence the geometric form but provide control over the speed of parametrization (see Figure 5). The importance of this phenomenon and some of its potential application will be discussed in Section 8.

A third important new observation about NUERBS concerns the geometry of its control polygon c_i in (6). Since for NUERBS the control polygon is non stationary, this theory is more interesting and more technical. For example, let us mention that the convex hull of the control polygon for $t \in [t_0, t_{n+1}]$ forms a tensor-product patch on a developable ruled surface. The theory of stability and condition number of the control polygon are more technical for NUERBS than for NURBS. The same holds for the theory of convergence of the control polygon in the case of knot refinement.

Another interesting topic is the theory of evolutes and evolvents of NUERBS.

Finally, let us mention that the expo-rational B-spline and NUERBS have very interesting properties per se in the complex-valued case, for both anisotropic and isotropic curves.

6. Tuning NUERBS by the Parameters of the Expo-Rational B-Splines

The basis function $B_k(t)$ (see equations (3) and (4)) spans 3 knots, i.e. 2 intervals (hence, at most 2 expo-rational B-splines are locally non-zero for any fixed t). In Figure 7 several examples of expo-rational basis functions and respective derivatives are given. In all examples in Figure 7 we have $\lambda = 0.5$. The three first examples in Figure 7 are symmetric. We call Example 1 default because all intrinsic parameters $\alpha, \beta, \gamma, \sigma$ on both sides are 1. In Example 2 both α and β are close to zero, and the result is close to a piecewise linear basis. In Example 3 $\alpha = \beta = 2$, $\gamma = 0.25$ and σ is close to zero. The result is close to a step function. Basis functions 4, 5 and 6 are all non-symmetric examples. In Figure 8 there is an example of using the basis function 2 from Figure 7. One can see the resulting "sharp" edge in the middle. If instead the B-spline basis of Example 6 (or 3) is used, it is possible to model approximation of discontinuities

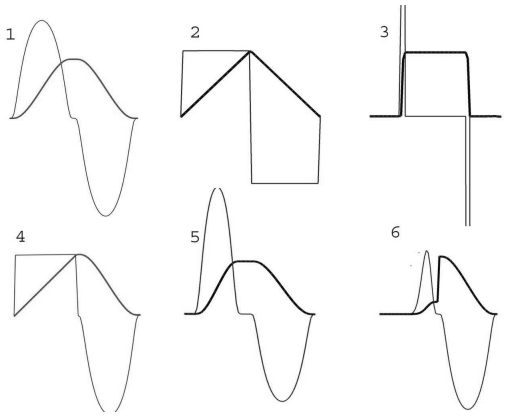

Figure 7: Examples of 6 different expo-rational basis functions where example 1 is the default because all parameters are 1. Number 2 and 3 are symmetric, while all the other have default values on right-hand side but not on the left-hand side (this is not an exhaustive list of all representative cases. See [2, 1, 6] for a more detailed list, including also variation of the parameter λ in (4))

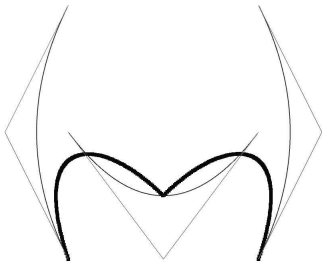

Figure 8: Example of a non-default intrinsic set of parameters. Basis function No. 2 in Figure 7 is used for blending the central one of the local curves, given with their respective control polygons (in red). Notice the "sharp" edge on the resulting global curve. Note also that the global curve is not regular in the center point, so theorem 2 fails

without losing the C^∞-smoothness of the expo-rational B-spline or NUERBS curve.

As a whole, this gives a diversified combined control over the NUERBS by tuning both the weights and the intrinsic parameters of the B-splines. It is of interest both for curves and surfaces and will be investigated in detail elsewhere (see [1] for an interpretation from the point of view of the duality between Voronoi tesselations and Delaunay triangulations, and their generalizations for dimensions higher then 2). The material of Section 5 also provided the important information that the expo-rational B-splines B_i, and the associated weights, W_i, *have no influence* over the intrinsic geometry of the curves in the knots t_k , $k = 1, ..., t_n$. Control over the curvature and torsion of the curve in the knot t_i can be achieved only via the coefficients and NUERBS weights of the local curve defined in $[t_{i-1}, t_{i+1}]$ (i.e., c_{ij} and w_{ij} in (16) and (18), in the case of polynomial-based local curves on $[t_{i-1}, t_{i+1}]$). On the other hand, on (t_{i-1}, t_i) and (t_i, t_{i+1}) both the intrinsic parameters of (the left-hand and right-hand side of) $B_i(t)$ and the weights $W_{i-1}, W_i, W_{i+1}, \vartheta_{i-1,j}, \vartheta_{i,j}, \vartheta_{i+1,j}$ and $\mu_{i-1,j}, \mu_{i,j}, \mu_{i+1,j}$ in (6), (17) and (18) do influence in a complex way the intrinsic geometry of the curve. This influence is of course related with the role of B_i as a blending function.

Remark. Statements analogous to the ones formulated here in Sections 5 and 6 about curves can also be formulated for the intrinsic geometry of tensor-product surfaces. We shall discuss this case in more detail elsewhere (see also [2, 1]).

7. Fundamentals of NUERBS Sampling Theory

As already pointed out, (7) implies that NUERBS are exact for all entire analytic functions on $[t_1, t_n]$. In [2, 1] this fact was used to prove some results on sampling with expo-rational B-splines. These results extend in a natural way to the case of NUERBS. Here we shall give as an example the immediate generalization of the result in [2, 1] to NUERBS.

Theorem 3. *Consider the infinite uniform mesh $t_i = i$, $i = 0, \pm 1, \pm 2, ...$ Let $f \in S(\mathbb{R})$ and assume that $g \in C^\infty(\mathbb{R})$ and, together with its derivatives of every order, $g(t)$ has polynomial growth as $t \to \pm\infty$. Assume also that $g(t) > 0$ for all $t \in \mathbb{R}$, and let $W_i = g(t_i)$ for all i. Then, the following sampling theorem*

holds

$$f(t)=\frac{\sum\limits_{i=-\infty}^{\infty}\left[\sum\limits_{j=0}^{\infty}\frac{(t-i)^j}{j!}f^{(j)}(i)\right]W_iB(t-i)}{\sum\limits_{i=-\infty}^{\infty}W_iB(t-i)} \tag{25}$$

for all $t\in\mathbb{R}$. *Moreover,* f *satisfies the following integral identity*

$$f(t)=\frac{\sum\limits_{j=0}^{\infty}\frac{1}{j!}\int_{-\infty}^{\infty}(t-\theta)^jf^{(j)}(\theta)g(\theta)B(t-\theta)d\theta}{\int_{-\infty}^{\infty}g(\theta)B(t-\theta)d\theta} \tag{26}$$

for all $t\in\mathbb{R}$.

Proof. (Outline) In this case (25) is (12), which is true, in view of (7). Applying the Euler-McLaurin expansion to the numerator and denominator of the RHS in (25) and taking in consideration the assumptions of the theorem yields (26). Note that (25) and (26) follow also directly from the Taylor analytic expansion of f for any fixed $\theta\in\mathbb{R}$:

$$f(t)=\sum_{j=0}^{\infty}\frac{1}{j!}(t-\theta)^jf^{(j)}(\theta). \qquad \square$$

Remark. Like the original sampling theorem for expo-rational B-splines in [2], Theorem 3 can under appropriate assumptions be extended to a non-uniform knot-vector $\{t_i\}, i=0,\pm1,\pm2,...$, the resulting integrals in (26) being Riemann-Stieltjes. Further extensions of (25) and (26) are possible in a weak sense when $f\in S'(\mathbb{R})$ and the Riemann-Stieltjes integral in (26) is consecutively extended to Lebesque-Stieltjes, and ultimately to the duality functional between $S(\mathbb{R})$ and $S'(\mathbb{R})$. This is achieved via standard continuity/density/completion argument, but the details are to technical to be addressed in this brief outline of proof.

Remark. A similar theorem can be formulated, more generally, for the general NUERBS form (6). Various enhancements can be obtained for particular cases of (6) and (13). In all cases, however, the main idea is the same as in Theorem 3.

Remark. Formulae of the type (25) and (26) have potential applications in analytic and numerical operational calculi where the choice of the weights, W_i, and the function g can be optimized with respect to customized criteria.

8. Applications

NUERBS are a new technique, and the range of its potential applications is vast (see [2, 1] for a more theoretically advanced exposition of 4 different model fields of potential applications). To begin with, NUERBS can outperform NURBS in the case of "difficult" spatially inhomogeneous curves and surfaces by providing a very flexible, yet infinitely smooth, solution. As shown by the example with Lagrange interpolation given above, as well as examples 3 and 6 in Figure 7, NUERBS self-adapts to follow even non-smooth shapes, leading to the much more efficient control over the speed of parametrization than in the case of NURBS. The reasons for this increased efficiency is that speeds and accelerations in an expo-rational curve can be much larger than in a polynomial-based curve, and that expo-rational B-splines are non-regular curves at the knots. This is also the reason why geometric continuity can be exploited much more efficiently with NUERBS than with NURBS.

From a computational point of view, expo-rational B-Splines and NUERBS are more expensive to compute than polynomial-based ones, but with every new generation of CPUs this difference is diminished, and already today it is fully compensated by the expo-rational B-spline's extreme localization of the support, in combination with its infinite smoothness.

One very important application of expo-rational B-splines and NUERBS arises in the approximate solution of operator equations with densely defined closed unbounded operators (ODE, PDE, singular integral and pseudo-differential equations). Note, for example, that the expo-rational Lagrange interpolation basis, which geometrically utilizes the piecewise-linear B-spline basis while retaining C^∞-smooth parametrization, can be used for solving ODE and PDE of *arbitrary order* (the resulting stiffness matrix remaining tri-diagonal). This means that at all times we have a "classical" C^∞-smooth approximate solution converging to the true solution of the PDE (whose solution may exist only in a weak sense). In this way we use to a maximal extent the fact that C^∞-smooth functions with compact support are dense in the distribution space $\mathbb{D}$ (including the space of moderate distributions S', see e.g. [8, 10].

Another application having the potential for considerable future impact is the use of expo-rational B-splines and NUERBS in numerical computational algorithms for the GPU, for numerical solutions of PDEs and for wavelet-based image processing. Moreover, we claim that expo-rational B-splines and NUERBS will vastly outperform B-splines and NURBS in algorithms for the GPU, for the following important reasons. The "GPU-computational paradigm" requires that when solving a PDE by finite element methods on the GPU, the

finite element basis has to be pre-computed (see [5]). In pre-computed form, the expo-rational and NUERBS bases retain all of their considerable advantages to B-splines and NURBS, while the computation of the former and the latter is done in exactly the same way (by using tables). In the case of wavelet processing on the GPU, a big advantage of expo-rational B-spline multi-wavelets is that they have also NUERBS form which can be used very efficiently, for instance, in processing non-negative images, e.g., for processing PET (positron-emission tomography) images in medical imaging of the brain, in particular, for brain image registration. In connection with image processing, let us note also that multilevel expo-rational B-splines and their NUERBS forms (organized as truncations of continuous fractions) offer an entirely new broad perspective. The NUERBS form of expo-rational B-spline multi-wavelets is one first important particular instance of the use of the multilevel NUERBS.

References

[1] L.T. Dechevsky, A. Lakså, B. Bang, Expo-rational B-splines, *Int. J. Pure Appl. Math.*, **27**, No. 3 (2006) 319-368.

[2] L.T. Dechevsky, A. Lakså, B. Bang, Expo-rational B-splines, *Preprint*, No. 1/2005, Applied Mathematics, Narvik University College, Norway, ISSN 1504-4653.

[3] L.T. Dechevsky, A. Lakså, B. Bang, NUERBS form of expo-rational B-splines, *Preprint*, No. 1/2004, Applied Mathematics, Narvik University College, Norway, ISSN 1504-4653.

[4] G. Farin, J. Hoschek, M.-S. Kim (Editors), *Handbook of Computer Aided Geometric Design*, Elsevier (North Holland) (2002).

[5] J.M. Hjelmervik, T.R. Hagen, GPU-based screen space tesselation, In: *Mathematical Methods for Curves and Surfaces, Tromsø, 2004* (Ed-s: M. Dæhlen, K. Mørken, L. Schumaker), Mod. Methods Math, Nashboro Press, Brentwood, TN (2005), 213-222.

[6] A. Lakså, B. Bang, L.T. Dechevsky, Exploring expo-rational B-splines for curves and surfaces, In: *Mathematical methods for Curves and Surfaces* (M. Dæhlen, K. Mørken, L. Schumaker), Tromsø(2004), 253-262; Mod. Methods Math., Nashboro Press, Brentwood, TN (2005).

[7] T. Lyche, K. Mørken, *Theory and Application of Splines*, Manuscript, Oslo University (1998).

[8] M. Reed, B. Simon, *Methods of Modern Mathematical Physics, Vol. 1: Functional Analysis*, Acad. Press (1972).

[9] I.J. Schoenberg, Monosplines and quadrature formulae, In: *Theory and Applications of Spline Functions, Madison Wisconsin 1968, Proceedings*, Acad. Press (1969), 157-207.

[10] V.S. Vladimirov, *Generalized Functions in Mathematical Physics,* Nauka (1979), In Russian.